Available online at www.sciencedirect.com
SCIENCE DIRECT®
Coordination Chemistry Reviews 248 (2004) 441–455
COORDINATION CHEMISTRY REVIEWS
www.elsevier.com/locate/ccr

Review

Studies on the mechanism of hydrolysis and polymerization of aluminum salts in aqueous solution: correlations between the "Core-links" model and "Cage-like" Keggin-Al_{13} model

Shuping Bi*, Chenyi Wang, Qing Cao, Caihua Zhang

Department of Chemistry, State Key Laboratory of Coordination Chemistry, Nanjing University, Nanjing 210093, China

Received 8 September 2003; accepted 24 November 2003

Contents

Abstract

Two conflicting models describe the mechanism of aluminum (Al) hydrolysis and polymerization in aqueous solution, namely, the "Core-links" model and the "Cage-like" Keggin-Al_{13} model. For the sake of simplicity, the expressions of Al_{13} in the "Core-links" model and the "Cage-like" model are termed as C-Al_{13} and K-Al_{13}, respectively. The two models have co-existed for almost 50 years, but describe differences in the transformation of polymeric Al speciation in aqueous solution, such as, hydrolysis, polymerization, flocculation, precipitation and crystallization. Many of the polynuclear Al species presented in the literature cannot be adequately described with either the "Core-links" model or the "Cage-like" Keggin-Al_{13} model. This paper introduces new considerations for the mechanism of Al hydrolysis and polymerization in aqueous solution, a "Continuous" model representing a unification of the "Core-links" model and "Cage-like" model,

*Corresponding author. Tel.: +11-86-25-86205840; fax: +11-86-83317761.
E-mail address: bisp@nju.edu.cn (S. Bi).

doi:10.1016/j.ccr.2003.11.001

based on the systematic summary and analysis of numerous published experimental results. The general viewpoints are:

(1) The "Core-links" model can only describe the transient state process for speciation changes of Al in hydrolysis and polymerization. Under a moderate titration rate of Al solution using alkaline solution, the transformation of polynuclear Al species in forced hydrolyzed Al solutions has gone through the continuous speciation change process: from small polymer (linear shape) → middle polymer (plane shape) → large polymer (stereoscopic conformation). This is a continuous transient course and can be described by the "Core-links" model.
(2) The "Cage-like" Keggin-Al_{13} model may only depict the metastable (sub-steady state) speciation of polynuclear Al, which is formed through the structural re-organization (self-assembly) during the aging of transient species. Aging is the prerequisite condition for the formation of K-Al_{13}. After aging the transient species of polymeric Al produced in titration, the concentration of polymeric Al determined by Ferron timed-spectrometry is equal to that of Al_{13} concentration measured by ^{27}Al-NMR, namely Al_b(photometry) ≈ K-Al_{13} (OH^-/Al = 1.0–2.8). So that the existence of K-Al_{13} is universally approved. However, the "Cage-like" K-Al_{13} structural model cannot explain the whole transformation process of polynuclear Al in aqueous solution, since many polymeric Al species produced in titration processes (transient state) cannot be detected by ^{27}Al-NMR. In addition, the slow base-neutralization and the moderate reaction atmosphere favors the polymeric Al, facilitating the formation of K-Al_{13} by self-assembly.
(3) The two models can be unified. They actually reflect the different stages of the Al speciation in hydrolysis and polymerization: Al^{3+} → "Core-links" species (transient state) → K-Al_{13} (metastable state) → Al(OH)$_3$(s, steady state) → $Al(OH)_4^-$. There is an inevitable intrinsic connection between the interesting polymeric Al_{13} species C-Al_{13} and K-Al_{13}. This connection can be summarized as C-Al_{13}^{9+} → K-Al_{13}^{7+}, which is an irreversible self-assembly course.
(4) The reason for the many seemingly inconsistent and even paradoxical literature reports is due to assessment at the different stages of the Al species chain in addition to differences in experimental conditions. Therefore, a combined "Continuous" model is presented to describe the linkage of "Core-links" model and "Cage-like" model. It is based on our newly introduced concept of experimental condition comprehensive parameter—"the flux of alkali neutralization Φ".

Keywords: Core-links model; Cage-like (Keggin-Al_{13} structure) model; Continuous model; Transformation of polynuclear aluminum species; Aluminum speciation chain

1. Introduction

Aluminum (Al) is the third most abundant element in the lithosphere, second only to oxygen and silicon, making up approximately 8.1% by weight in soil. Because of its extensive availability and special chemical properties, Al is present in soil solutions and natural waters in the form of monomeric, polymeric, sol/gel and sediment, depending on the composition of the mineral phase, the base saturation of soil, the pH, adsorption, as well as complexation with different inorganic and organic ligands [1–4]. In partially neutralized Al^{3+} solutions, the hydrolysis–polymerization species of Al in dynamic equilibria also depend on the concentrations of Al^{3+} and base, the pH, the stirring strength, the temperature, the rate of base injection, and aging time, etc. The increasing concentration of Al in natural waters and soil solutions, resulting from the serious problem of acid deposition and acidic-mine drainage into the environment, has been reported to be poisonous to fish, marine bacteria, and plants [5–8]. The chemical behavior of Al in complex ecosystems or living organisms, its toxicity and reactivity or bioavailability, depends mainly on its chemical forms. Polynuclear hydroxo-Al complexes are much more phytotoxic than the hexahydrated ion or mononuclear hydroxo-Al complexes [9]: (1) polynuclear hydroxo-Al complexes play important environmental ecological roles in the hydrosphere. With the complex reactions of aquatic Al^{3+} taking place on the interfaces of minerals/water or in waters, they can influence the biogeochemical cycling of other elements on the planet through such physicochemical reactions as hydrolysis, polymerization, flocculation, precipitation, adsorption, complexation and electroneutralization; (2) they can decrease heavy metal mobility [3], and can also concentrate the toxic heavy metals (such as Cd, Cu and Zn, etc.) on the rhizosphere by adsorption, electroneutralization, enmeshing, and inhibit the elongation of the roots of several plants; (3) for humans, polymeric and monomeric Al species are well known for their toxicity to uremia patients [10,11], and the agent that contains Al (such as Ulcerlmin) has been used in curing the helcosis of stomach and duodenum. Particular concerns with regard to the increased concentration of polymeric Al have been raised in recent years, which come from coagulant (such as polynuclear Al chloride, polynuclear Al sulfate, polynuclear Al sulfate silicate, etc.) in the treatment of wastewater, especially potable water, and from boiling water using Al utensils [12]. There are important pathogenic synergistic factors causing bone loss, Alzheimer's disease (AD), Parkinson's disease (PD), Amyotrophic lateral sclerosis (ALS), and so on [13]. On the other hand, polymeric hydroxyl Al species in the nanosize have many industrial applications [14–21], such as coagulants in potable and waste water treatments, catalyst supports, clay stabilizing agent in oilfield, oil/water separating agents, cement quick condensation agents, binding agents of fire-resistant material, and the cloth anti-fold agents, etc. All of these increase the opportunities for Al entering the human body. Therefore, it is very important to study the transformation mechanisms of the hydrolysis–polymerization of Al^{3+} species in aqueous solution systems.

People have extensively explored the hydrolysis–polymerization mechanism and species conversions of Al^{3+} for a century. Many analytical methods have been used

in characterizing and quantifying polynuclear hydroxyl Al. But, up to now, there is still no agreement on the hydrolysis–polymerization reaction mechanism and the species conversion process [2,15,22]. The "Core-links" model and the "Cage-like" (Keggin-Al_{13}) model for hydrolysis–polymerization of Al^{3+} have coexisted for nearly 50 years despite some conflicts. The reasons for the inconsistent conclusions include the complexity of the hydrolysis systems, the deficiency of dynamic information and the different interpretations of the experimental data. The failure to describe the hydrolytic reactions and species conversions of Al^{3+} successfully in relatively simplified aqueous solutions has not only inhibited the development of present environmental Al chemistry, the extensive research on organic Al chemistry, and Al coordination chemistry in water solutions, but also confined the application of Al chemistry in different fields involved in aquatic life, sediment, soil systems, and water treatment industry. Therefore, establishing the mechanism of Al^{3+} hydrolysis–polymerization and its species distribution and conversion is very useful to understand the toxicity of aluminum, its bioavailability in the natural environment, the self-purification potential of natural water, and the industrial applications efficient of polynuclear Al. It is also an important theoretical basis to develop high efficiency flocculants [23].

The objective of the present paper are to: (1) give a fundamental summary of the hydrolysis–polymerization reactions of Al^{3+} in aqueous solutions; (2) discuss the formation mechanism of monomeric, polymeric, and sol/gel Al species, their distribution and transformation laws; (3) analyze the application conditions, the adaptability, and the inner connection of the two models of Al hydrolysis–polymerization; (4) put forward a "Continuous" model for the mechanism of the hydrolysis–polymerization of Al^{3+} to unify the "Core-links" model and the "Cage-like" Keggin Al_{13} model, and give some constructive suggestions.

2. The formation of hydroxyl and polynuclear Al: an historical perspective

Over the past 100 years, scientists have been carrying out extensive experimental research and model calculations on the speciation and the mechanism of the hydrolysis–polymerization of Al^{3+} [24–41]. A great deal of progress has been made. But the reports concerning the hydrolysis–polymerization species of Al^{3+} are disorganized. Furthermore, there is no unification between the two widely accepted models, the "Core-links" model and the "Cage-like" Keggin-Al_{13} model. Research into the hydrolysis–polymerization of Al^{3+} in aqueous solution, is still very active and contentious, following the guidelines of these two models.

2.1. The "Core-links" model

In 1952, Brosset [42] interpreted his experimental data successfully for the first time using potentiometric titrations and chemical modeling, and put forward an early form of the "Core-links" model. In 1954, Brosset et al. [43] suggested a series of "Core-links" polymeric Al species whose form is $Al(Al_2(OH)_5)_n{}^{3+n}$. Almost at the same time, Sillen [44] put forward a theoretical "Core-links" model. Afterwards, Hsu and coworkers [45,46]and Stol et al. [47] introduced and improved a "gibbsite-fragment" model or "hexameric ring scheme". The Brosset's "Core-links" model and the "gibbsite-fragment" model, developed together, formed the present "Core-links" model. It gives a distribution of continuously changed species from Al hydrolysis–polymerization production, thinking that the hydroxyl Al changes from monomer to polymer following the hexameric ring model. Its sol state can reach $Al_{54}(OH)_{144}{}^{18+}$ and then forms the gel precipitation $[Al(OH)_3]_n$ which maintains the sheet structure of gibbsite or bayerite (Fig. 1). In other words, the structure of OH–Al polymer in solution is the same as that of $Al(OH)_3$ [48,49], whose basic units are either $Al_6(OH)_{12}(H_2O)_{12}{}^{6+}$ (single hexamer ring) [50] or $Al_{10}(OH)_{22}(H_2O)_{16}{}^{8+}$ (double hexamer rings) [51] (see Fig. 2). This model cannot only interpret the various polymeric Al species, but also explains how the monomeric Al and polymeric Al are converted into $Al(OH)_3$(am). This "Core-links" model, despite scarcely considering its structure and lacking direct doubtless evidence to prove its existence, still remains the dominant position especially in the field of geochemistry because it follows the crystallographic law of gibbsite. Many scholars remain strong supporters of the model [52], so that it has been coexisting with the "Cage-like" Keggin-Al_{13} model for more than 50 years.

2.2. The "Cage-like" (Keggin-Al_{13} structure) model

The Keggin-Al_{13} polynuclear species was first proposed by Johansson [53–55]. It is formed through sulfate precipitated from partially neutralized Al^{3+} solutions that were

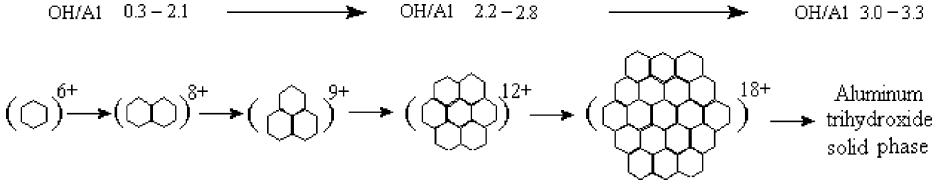

Fig. 1. The polymerization of Al^{3+} via coalescence of the hexamer units according to the "gibbsite-fragment" model [2,51].

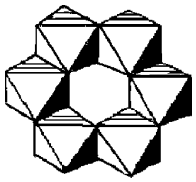

Fig. 2. The basic structure of the hexamer units model $Al_6(OH)_{12}(H_2O)_{12}{}^{6+}$ [50].

heated 30 min at 80 °C and aged for a few days. Rausch and Bale [56] have further verified the existence of Keggin-Al_{13} in partially neutralized Al^{3+} solutions of $\tilde{n} = 1.5$–2.25 ($\tilde{n}$ is the OH/Al mol ratio) that were heated 1 h at 70 °C by the aid of small angle X-ray scattering. The structural analysis shows that this tridecamer can be visualized as having a central tetrahedral AlO_4 core, surrounded by 12 Al octahedral AlO_6 units in the form of a cage (Fig. 3). So, it can be described as $AlO_4Al_{12}(OH)_{24}(H_2O)_{12}{}^{7+}$, which is usually called "Cage-like" Keggin Al_{13} structure. This model holds that in Al solution there are only monomer, dimer, Keggin-Al_{13} polymer, and larger polymerized Al species. These species can be transformed from one to another directly [57–59]. Since the polynuclear species of Al^{3+} in the "Cage-like" model can be identified instrumentally, this model has gained more approval and become the main viewpoint in the chemistry of flocculant [59–62]. However, it can only monitor four highly symmetric Al species by ^{27}Al-NMR studies, whose chemical shifts follow as: hexaaqua Al^{3+} and monomer, $Al(H_2O)_6{}^{3+}$, $Al(OH)(H_2O)_5{}^{2+}$ and $Al(OH)_2(H_2O)_4{}^{+}$, at 0 ppm; dimer, $Al_2(OH)_2(H_2O)_8{}^{4+}$ and few trimer $Al_3(OH)_4(H_2O)_{10}{}^{5+}$, at 3–5 ppm; the tridecamer, $AlO_4Al_{12}(OH)_{24}(H_2O)_{12}{}^{7+}$ or Keggin-Al_{13}, at 62.5 ppm; and the $Al(OH)_4{}^{-}$ anion assigned at 80 ppm, in which only the tetradentate Al^{3+} ion, in symmetric environment, can bring about the resonant peak. A signal is not observed for the hexadentate Al^{3+} ion in non-symmetric environment. For the polymeric Al solution with high basicity ($\tilde{n} > 2.0$), it is hard to distinguish Al_2 and Al_3 and the integration quantifies these four Al species.

2.3. The argument between two models

There have been many drastic arguments in the past 50 years between the "Core-links" model and the "Cage-like" Keggin-Al_{13} model about the formation of polynuclear Al [63–66]. The argument mainly focuses on two aspects:

(1) What are the primary species of hydrolytic products in the partially hydrolyzed Al solutions → Keggin-Al_{13} model is based on experimental results of ^{27}Al-NMR and X-ray scattering, but it can explain neither the polymerization process of Al^{3+} salts solution nor the formation process of numerous metastable polymeric Al species and sediment Al_c, including the formation of Keggin-Al_{13} itself. On the other hand, although the "Core-links" model is consistent with the experimental results of potentiometric titration, it cannot explain the formation process and the structure of $Al_{13}O_4(OH)_{24}{}^{7+}$.
(2) How are the two models interrelated? How can these two models be turned into sheet structure $Al(OH)_3$ of the "gibbsite-fragment" model (hexamer species) through variant channel?

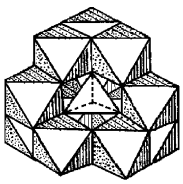

$[\,AlO_4Al_{12}(OH)_{24}(H_2O)_{12}]^{7+}$

Fig. 3. The basic structure of the Al_{13} in Keggin-Al_{13} model [50].

In the past 50 years, people have been attempting to clarify these relations. Hsu and coworkers, the supporter of the "Core-links" model, found that two completely different base Al sulfate (amorphous and crystallization) were formed when Na_2SO_4 was put into freshly prepared and aged polymeric Al solutions respectively [14,15,45,46,49,51,67]. From this, it is obviously that neither of these two models is adequate to describe the polynuclear OH–Al complexes in solution. Actually, the Keggin-Al_{13} model is mainly deduced from the identification of ^{27}Al-NMR [57] and small angle X-ray diffraction [54,56]. Among various analytical technologies confirming the presence of Al hydrolysis products, ^{27}Al-NMR spectroscopy is a fast, direct technique for tracing the change in Al species with variations in pH [68], and is widely applied to hydrolysis of Al, Al complexation, quantitative test and species analysis. It offers some important information for the types of polymeric Al and the species distribution of monomeric Al and polymeric Al. It can also provide an insight into the Al species interacting with organic and inorganic ligands and offers both quantitative and structural information. However, it lacks selectivity and sensitivity [69], partly due to its spectral line broadening of the low symmetric species [70], and partly due to the disturbance of background [69]. Actually, a lot of polymeric Al species can't be detected by ^{27}Al-NMR, so those species that can't be detected directly by experiments may also exist. Those species that are detected by ^{27}Al-NMR are only the species of certain stage of the hydrolysis–polymerization of Al^{3+}. Under some conditions, they are probably all composed of Al (Al_T), but under other conditions, they only take a small part of Al_T, even under 50% [57]. The invisible parts of ^{27}Al-NMR spectrum sometimes make the peak base greatly wider without confirming their forms. These species seem to contain polymers of tetrahedra [64], that are higher than Al_{13}, or Al_{13} aggregation whose form is colloidal and/or precipitate [34,67,70–76], but there are suggestions that they contain oligomers of Al_2–Al_{12} [57,59,73].

3. The formation process of transient and metastable polynuclear Al species: our thoughts

The transformation of polynuclear Al species in the course of "hydrolysis–polymerization–flocculation–precipitation–crystallization" of soluble Al occurring in aqueous systems is a hot issue with plenty of historical documents. Especially, it is hard to unify the arguments for its intermediate hydrolysis. The species of polynuclear Al described in the literature are scattered and confusing, and cannot be described completely by the existing "Core-links" model or "Cage-like" Keggin-Al_{13} model. The contradictory source that two structural models cannot be mutually explained lies in the difference of their experimental conditions. This relation between transient polymeric Al and stable Keggin-Al_{13} is a universally neglected phenomenon. After having studied systematically the formation and species conversion of polynuclear Al in aqueous solution from lots of literature, we hereby establish a new combined "Continuous" model. It can describe the entire formation process of transient and metastable polynuclear Al species in aqueous solution. Table 1 gives the brief description and the comparison of these three models. In the following sections, we will describe this "Continuous" model in detail.

3.1. The hydrolysis and polymerization process of Al^{3+} described by the "Core-links" model

3.1.1. The fraction and distribution of polynuclear hydroxyl Al species

Referring to the potentiometric titration experimental method and under the moderate rate of base injection (titration rate is in the range of 0.5–1.5 ml/min) [86], we expounded that there are six characteristic points on the base titration curve when using base to titrate Al solutions: three critical points and three inflection points (see Fig. 4). The changes of characteristic points reflect the influence of experimental conditions in the course of the hydrolysis–polymerization and the conversion of polynuclear hydroxy Al species. Six characteristic points are obtained from potentiometric titration curve. Among them the critical point is the crossing point of two neighboring tangent lines passing through the inflection point, while the inflection point is where the second derivative's value is zero on potentiometry curve equation. The three critical points are noted as A($\tilde{n}_A$, pH_A), B($\tilde{n}_B$, pH_B) and C($\tilde{n}_C$, pH_C), respectively ($\tilde{n}$ is defined as OH/Al mol ra-

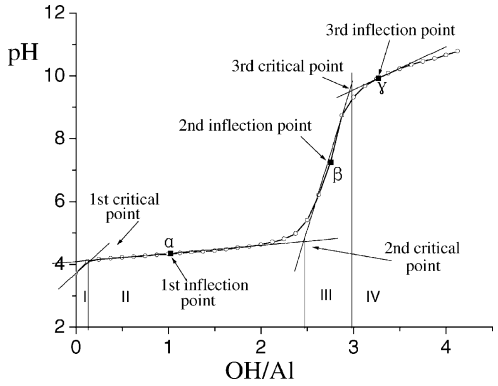

Fig. 4. The base titration curve (pH vs. OH/Al) and the fractionation of polynuclear Al under the moderate low rate of base addition (four districts/six characteristic points). Titration rate = 0.8 ml/min, $AlCl_3 = 5 \times 10^{-3}$ M, NaOH = 0.01 M, ionic strength $I = 2 \times 10^{-2}$ M.

Table 1
The brief description and comparison of the three models

Model	Brief description
"Core-links"	(1) It gives a distribution of the continuously changed transient state model species of Al in hydrolysis–polymerization process. It can interpret the various possibly existing and instantaneously existing polymeric Al species, and explain the experimental facts about how the monomeric and polymeric Al are converted into $Al(OH)_3$(am). But it lacks direct and unequivocal evidence to prove the existence of these transient species (2) The hydroxyl Al changes from monomer to polymer following the hexameric ring model. The structure of OH–Al polymer in solution is the same as that of $Al(OH)_3$, whose basic units either $Al_6(OH)_{12}(H_2O)_{12}^{6+}$ (single hexamer ring) or $Al_{10}(OH)_{22}(H_2O)_{16}^{8+}$ (double hexamer rings) (3) Under the condition of moderate rate of base injection titrating Al^{3+} salts
"Cage-like"	(1) In Al solution there are only monomer, dimer, Keggin-Al_{13} polymer, and model larger polymerized Al species. These species can be transformed from one to another directly (2) The metastable K-Al_{13} is formed by the structural reshuffle of transient species after aging. The changing process is the transient polymeric Al from disorder to order, based on results of ^{27}Al-NMR (3) Under the condition of aging, heating/adding extra SO_4^{2-} and slow rate of injecting base
"Continuous"	(1) Polynuclear Al species are actually a series of dynamic intermediates formed in the process of "hydrolysis–polymerization–flocculation–sediment" (2) The polymeric Al_b is not the mixture of many polymeric Al forms in the aged polymeric Al solutions. Under the fixed mol ratio of OH/Al, if prolonging the aging time properly, only one polymeric Al species may take the absolute percentages. This kind of form is just K-Al_{13} (3) The metastable K-Al_{13} is formed by the structural reshuffle of transient species after aging. Aging is one prerequisite for K-Al_{13} Bformation; Elevating temperature and addition of extra SO_4^{2-} promote this conversion process (4) It is a combined model unifiying the "Core-links" model and "Cage-like" model. It can explain the entire hydrolysis-polymerisation course using OH^- titrating Al^{3+} solution with the concept of alkali flux neutralization Φ

tio). The three critical points (or A, B, C) express different meanings: At A ($\tilde{n} = 0.2$), mononuclear Al begins to convert into small/middle polynuclear Al; At B ($\tilde{n} = 2.5$), the small/middle polynuclear Al begins to form the large polynuclear Al; At C ($\tilde{n} = 3.0$), the amorphous gel or sediment begins to dissolve. The meanings of three inflection points are: at α ($\tilde{n} = 1.0$), small polymeric Al will change into medium-sized polymeric Al; at β ($\tilde{n} = 2.8$), large polymeric Al will change into gel or sediment; at γ ($\tilde{n} = 3.3$), $Al(OH)_3$ (aq or am) will dissolve as $Al(OH)_4^-$. According to the OH/Al mol ratio, the OH/Al versus pH curve in the absence of complexing ligands other than OH^- can be quantitatively divided into four districts by the three critical points. Following is the detailed statement:

(1) District I ($\tilde{n} < 0.2$, pH = 4.1): the main Al species are Al^{3+} and monomeric Al. The value of $\tilde{n}$ greatly affects the distribution of Al species in the solution of Al^{3+}. The acidity of the initial Al^{3+} solution maintains the free ion or monomeric species Al^{3+}, $Al(OH)^{2+}$, $Al(OH)_2^+$, and $Al(OH)_3^0$(aq). Fig. 4 indicates that $\tilde{n} = 0.2$ (the first critical point) is the threshold value of OH/Al, and the main Al species is mononuclear Al (or Al_a) under pH 4.1.

(2) District II ($0.2 < \tilde{n} < 2.5$, $4.1 <$ pH < 4.6): the main Al species are small/middle polymeric Al. Mononuclear Al forms OH–Al polymer to give Al_2–Al_{12} species [43,87,88], such as $Al_2(OH)_4^{2+}$, $Al_3(OH)_4^{5+}$, $Al_4(OH)_8^{4+}$, $Al_5(OH)_{13}^{2+}$, $Al_6(OH)_{12}^{6+}$, and $Al_{10}(OH)_{22}^{8+}$. They are characterized by low polymerization, medium charge, and ease of polymerization. Fig. 4 shows a small pH range between $0.2 < \tilde{n} < 2.5$ in the acid–base titration [47], as OH^- is almost all used for polymerization assuming the formation of $Al_m(OH)_{\tilde{n}m}^{(3m-\tilde{n}m)+}$ species, where the $\tilde{n}$ is mol ratio of OH/Al, $m \geq 2$, m and $(3m - \tilde{n}m)$ are integers. In this district, the experimental curve is almost a continuous horizontal line, which indicates that the polymerization rate of the small-size/middle-size polymeric Al is fast [47]and continuous. The smaller $\tilde{n}$ is, the more monomeric Al, and the less polymeric Al and sol/gel sediment. With increasing $\tilde{n}$, the volume of polymeric Al dominates, developing a panel shape, and sol Al_c.

(3) District III ($2.5 < \tilde{n} < 3.0$): the main Al species are large polymeric Al and sol/gel $Al(OH)_3$. Mononuclear Al decreases substantially in favour of larger polymer [52], whose main species are Al_{13}–Al_{54}, including $Al_{13}(OH)_{32}^{7+}$, $Al_{13}(OH)_{34}^{5+}$, $Al_{14}(OH)_{32}^{10+}$, $Al_{14}(OH)_{34}^{8+}$, $Al_{15}(OH)_{30}^{15+}$, $Al_{15}(OH)_{36}^{9+}$, $Al_{15}(OH)_{37}^{8+}$, $Al_{18}(OH)_{42}^{12+}$, $Al_{16}(OH)_{38}^{10+}$, $Al_{24}(OH)_{48}^{24+}$, $Al_{24}(OH)_{60}^{12+}$, $Al_{30}(OH)_{58}^{32+}$, $Al_{30}O_8(OH)_{56}^{18+}$, $Al_{42}(OH)_{108}^{18+}$, $Al_{54}(OH)_{144}^{18+}$. The rate of polymerization or depolymerization is very slow, so that addition of OH^- raises the pH. Hydrogen bonding and Van der Waals forces, the dimension of polymeric Al is no longer confined in planar fabric [59,89]. Up to $\tilde{n} = 2.8$ ($\tilde{n} = 2.8$ is the second inflection point), the entire solution is still acid or near neutral, OH–Al polymer still has a little positive charge [63], without precipitation. After the inflection point of $\tilde{n} = 2.8$, the $\tilde{n}$ range is so narrow that sol/gel or undefined sediment is generated in large quantities [23], and when $\tilde{n} > 2.8$, the formation rate of Al_c is accelerated.

In some literature, the Al species after $\tilde{n} > 2.5$ are considered as $Al(OH)_3$ sediment, while $\tilde{n} = 2.5$ is a characteristic point to form large polymeric Al in other literature [90]. In the range of $\tilde{n} = 2.5$–2.8, the pH rises sharply when adding OH^-, and decreases sharply while adding H^+, and the pH drift in this range is consistent with the slow formation or rearrangement of polynuclear structures [52], and also indicates the hydrolyzed polymeric Al is stable in this district [47,52]. At the isoelectric point, further combination with –OH or –O gives sediment on the surface [23], and coagulation forms visible amorphous gel sediment $Al(OH)_3$. Shen and Dempsey [91] have also detected some important larger and more steady polymeric Al including Al_{13} by the potential titration technique and Ferron assaying.

(4) District IV ($\tilde{n} > 3.0$, pH = 9.6): the district of the gel Al_c and then monomeric $Al(OH)_4^-$. The positive charge on the surface of hydroxyl polynuclear Al is very weak and the gel Al_c begins to dissolve and form $Al(OH)_4^-$.

In conclusion, the small species of hydroxyl polynuclear Al are stable in acid solution, but the large species of hydroxyl polynuclear Al only exist in neutral or weak base. The titration curve reflects the transient polymeric Al species. The results that come from Al-Ferron assaying, model the derivations of critical points and inflection points about the titration curve given by many researchers have verified the correctness of the partition of Al forms. The fraction and distribution of hydroxyl Al species are consistent with those reported [47,48,52,86].

3.1.2. The description for the features of various existing polynuclear Al species

Jander and Winkel [92] were the first to suggest the existence of polynuclear Al species based on diffusion coefficients measured in solutions of basic Al salts. Twenty years later, Brosset [42] found that the simple monomeric hydrolysis scheme was inappropriate for interpreting his potentiometric titrations of aqueous Al^{3+} solutions, and is better considered in terms of a series of indefinite polynuclear complexes. Lu et al. [93] also considered that a series of Al hydrolysis products of monomers and polymers were formed with varied $\tilde{n}$ or the pH in Al^{3+} solution. These species are coincident with the "Core-links" model. In short, we think, under the moderate rate of titration and violent stirring conditions, the species' change in the forced hydrolysis polymerization of Al salts is a continuous transient process. Each kind of transient polymeric Al species (Fig. 5) may exist under certain condition. Some corresponding equilibrium reactions and thermodynamic equilibrium

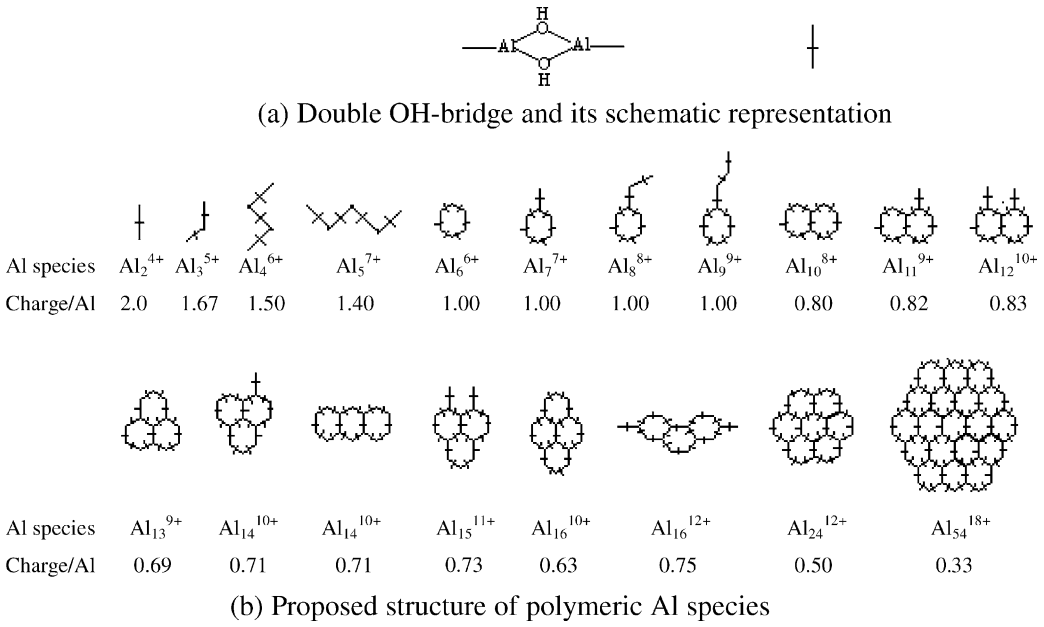

Fig. 5. The proposed structures for some possible existing polymeric Al species [2,22,47,49,52].

constants related to polynuclear Al are also given in literature [22,31,33,79,94,95].

3.1.3. The general summary for the regulation of hydroxyl Al species during the base titration of Al^{3+}

The "Core-links" model is an extensive concept, but few hexamer-ring species have been considered. Combining experimental results with the discussions above, we summarize the regulation of hydroxyl Al(III) species during the base titration of Al^{3+} as follows:

(1) The hydrolysis–polymerization process of Al^{3+} is continuous from small polymer → middle polymer → big polymer, and from linear shape → panel shape → stereoscopic conformations: (a) the linear shape polymeric Al is a small chain structure in which some octahedrons share one side through two hydroxyl bridges, including Al_2–Al_5 species, which are the initial polymers forms. They are unstable and are converted to panel and stereoscopic conformations; (b) the forms of the polymeric Al after Al_5 transform directly into a panel structure. All are medium-sized polymeric Al species, including Al_6–Al_{12} species. They employ hexameric rings as a skeleton and form a two-dimensional layer structure through the connection of skeleton and branching chains; (c) at higher pH, the surface positive charge is reduced, the hydroxyl bridges in polymeric Al are converted into oxygen bridges, preventing polymeric Al molecules. Each panel shape polymer can be changed into stereoscopic conformations under proper condition with aging. We classify these forms as the big polymeric Al bodies, mainly including Al_{13}–Al_{54} species; (d) stereoscopic conformations form through the nestification of flaky polymer layer by layer, or through the aggregation of "Al_{13} units". The panel forms are produced in the course of titration, while the big polymeric Al with stereoscopic conformation can only be produced in the aged partially hydrolyzed Al solutions.

(2) The addition of OH^- will alter the surface electromotive force of polymeric Al micelle, thereby influencing the stability of polymeric Al colloid. Because the polymeric Al body after Al_{54} is larger in size, and its pH accesses to the isoelectric point of $Al(OH)_3$ (the pH in minimum solubility), each aggregate has low stability. The polymerization process is generally interrupted by the precipitation of Al hydroxides. Hydrogen bonding, van der Waals forces, and self-assembly of polymeric Al between the layers of the panel form of polymeric Al, gives stereoscopic conformations.

(3) Under the forced hydrolysis conditions in which OH^- is injected continuously, the polymeric Al form is hydroxyl saturated and the coordination number of structural hydroxyl-groups is variable. Polymeric Al changes from polymer to the amphiprotic and zero valency $[Al(OH)_3]_n$ (aq.), which has the same degree of polymerization, and is then changed into large polymer after adsorbing OH^- on the surface of $[Al(OH)_3]_n$ (aq.). The number of heart Al^{3+} ion depends on pH difference and Al^{3+} concentration, while the specific form and the change of form depend on experimental conditions, such as, concentration, temperature, the rate of injecting the base, the stirring strength and aging time, etc. But under the specific $\tilde{n}$, the polymer is unique. The more stable "Core-links" species is $[Al_m(OH)_{\tilde{n}m}]^{(3m-\tilde{n}m)+}$ ($1.0 < \tilde{n} < 2.8$). This extended "Core-links" model can better explain why the pH does not change when $\tilde{n} < 2.5$, but increases quickly when $\tilde{n} > 2.5$, and why

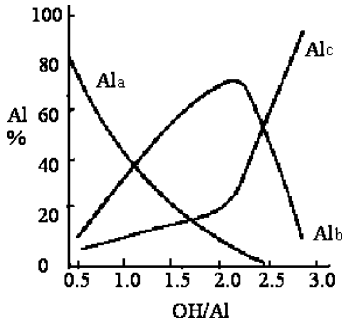

Fig. 6. The distribution of hydrolyzed species for polyaluminum as a function of OH/Al mol ratio value ($Al_T = 0.5$ M, 25 °C) [37].

there is still gel Al_c at low $\tilde{n}$, and monomeric Al_a at high $\tilde{n}$ (see Fig. 6). So, it is anastomotic to the experimental results of the photometric analysis, potentiometric titration analysis and the traditional "Core-links" theory.

(4) A general formula for all possible existing polynuclear species $Al_m(OH)_n(H_2O)_{4m+2-2u}^{(3m-n)+}$ includes a degree of unsaturation, u (for panel shape polyaluminum u is the number of rings). The effective range of n is given in $(m-1)\times 2 + 2u \le n \le 3m$ and Table 2.

3.2. The self-assembly of transient polymeric Al species and the formation of metastable Keggin-Al_{13} in partially neutralized Al(III) solutions

Researchers have shown that the metastable K-Al_{13} may result from the structural reshuffle of the transient polymeric Al species in the course of aging instead of the involvement of further hydrolysis. It must be aged firstly for transient polymeric Al species to be changed into metastable K-Al_{13}. Elevated temperatures and extra sulfate radical promotes this conversion indicating a connection be-

Table 2
The general formula for all possible polymeric Al species (N = number of species)

m	Code	Shape	General formula	N	Possible species
1	Al_1	Monomeric	$Al(OH)_n(H_2O)_{6-n}^{(3-n)+}$ (n = 0–3)	4	$Al(H_2O)_6^{3+}$–$Al(OH)_3(H_2O)_3^0$
2	Al_2	Linear	$Al_2(OH)_n(H_2O)_{10-n}^{(6-n)+}$ (n = 2–6)	5	$Al_2(OH)_2(H_2O)_8^{4+}$–$Al_2(OH)_6(H_2O)_4^0$
3	Al_3	Linear	$Al_3(OH)_n(H_2O)_{14-n}^{(9-n)+}$ (n = 4–9)	6	$Al_3(OH)_4(H_2O)_{10}^{5+}$–$Al_3(OH)_9(H_2O)_5^0$
	Al_3	Single ring	$Al_3(OH)_n(H_2O)_{12-n}^{(9-n)+}$ (n = 6–9)	4	$Al_3(OH)_6(H_2O)_6^{3+}$–$Al_3(OH)_9(H_2O)_3^0$
4	Al_4	Linear	$Al_4(OH)_n(H_2O)_{18-n}^{(12-n)+}$ (n = 6–12)	7	$Al_4(OH)_6(H_2O)_{12}^{6+}$–$Al_4(OH)_{12}(H_2O)_6^0$
	Al_4	Single ring	$Al_4(OH)_n(H_2O)_{16-n}^{(12-n)+}$ (n = 8–12)	5	$Al_4(OH)_6(H_2O)_{12}^{6+}$–$Al_4(OH)_{12}(H_2O)_6^0$
5	Al_5	Linear	$Al_5(OH)_n(H_2O)_{22-n}^{(15-n)+}$ (n = 8–15)	8	$Al_5(OH)_8(H_2O)_{14}^{7+}$–$Al_5(OH)_{15}(H_2O)_7^0$
	Al_5	Single ring	$Al_5(OH)_n(H_2O)_{20-n}^{(15-n)+}$ (n = 10–15)	6	$Al_5(OH)_{10}(H_2O)_{10}^{5+}$–$Al_5(OH)_{15}(H_2O)_5^0$
6	Al_6	Single ring	$Al_6(OH)_n(H_2O)_{24-n}^{(18-n)+}$ (n = 12–18)	7	$Al_6(OH)_{12}(H_2O)_{12}^{6+}$–$Al_6(OH)_{18}(H_2O)_6^0$
7	Al_7	Single ring	$Al_7(OH)_n(H_2O)_{28-n}^{(21-n)+}$ (n = 14–21)	8	$Al_7(OH)_{14}(H_2O)_{14}^{7+}$–$Al_7(OH)_{21}(H_2O)_7^0$
8	Al_8	Single ring	$Al_8(OH)_n(H_2O)_{32-n}^{(24-n)+}$ (n = 16–24)	9	$Al_8(OH)_{16}(H_2O)_{16}^{8+}$–$Al_8(OH)_{24}(H_2O)_8^0$
9	Al_9	Single ring	$Al_9(OH)_n(H_2O)_{36-n}^{(27-n)+}$ (n = 18–27)	10	$Al_9(OH)_{18}(H_2O)_{18}^{9+}$–$Al_9(OH)_{27}(H_2O)_9^0$
10	Al_{10}	Double ring	$Al_{10}(OH)_n(H_2O)_{38-n}^{(30-n)+}$ (n = 22–30)	9	$Al_{10}(OH)_{22}(H_2O)_{16}^{8+}$–$Al_{10}(OH)_{30}(H_2O)_8^0$
11	Al_{11}	Double ring	$Al_{11}(OH)_n(H_2O)_{42-n}^{(33-n)+}$ (n = 24–33)	10	$Al_{11}(OH)_{24}(H_2O)_{18}^{9+}$–$Al_{11}(OH)_{33}(H_2O)_9^0$
12	Al_{12}	Double ring	$Al_{12}(OH)_n(H_2O)_{46-n}^{(36-n)+}$ (n = 26–36)	11	$Al_{12}(OH)_{26}(H_2O)_{20}^{10+}$–$Al_{12}(OH)_{36}(H_2O)_{10}^0$
13	Al_{13}	Triple ring	$Al_{13}(OH)_n(H_2O)_{48-n}^{(39-n)+}$ (n = 30–39)	10	$Al_{13}(OH)_{30}(H_2O)_{18}^{9+}$–$Al_{13}(OH)_{39}(H_2O)_7^0$
	Al_{13}	Keggin	$Al_{13}O_4(OH)_n(H_2O)_{32-n}^{(31-n)+}$ (n = 24–31)	8	$Al_{13}O_4(OH)_{24}(H_2O)_8^{7+}$–$Al_{13}O_4(OH)_{31}(H_2O)^0$
14	Al_{14}	Triple ring	$Al_{14}(OH)_n(H_2O)_{52-n}^{(42-n)+}$ (n = 32–42)	11	$Al_{14}(OH)_{32}(H_2O)_{20}^{10+}$–$Al_{14}(OH)_{42}(H_2O)_8^0$
15	Al_{15}	Triple ring	$Al_{15}(OH)_n(H_2O)_{56-n}^{(45-n)+}$ (n = 34–45)	12	$Al_{15}(OH)_{34}(H_2O)_{22}^{11+}$–$Al_{15}(OH)_{45}(H_2O)_9^0$
16	Al_{16}	4-ring	$Al_{16}(OH)_n(H_2O)_{58-n}^{(48-n)+}$ (n = 38–48)	11	$Al_{16}(OH)_{38}(H_2O)_{20}^{10+}$–$Al_{16}(OH)_{48}(H_2O)_{10}^0$
17	Al_{17}	4-ring	$Al_{17}(OH)_n(H_2O)_{62-n}^{(51-n)+}$ (n = 40–51)	12	$Al_{17}(OH)_{40}(H_2O)_{22}^{11+}$–$Al_{17}(OH)_{51}(H_2O)_{11}^0$
18	Al_{18}	4-ring	$Al_{18}(OH)_n(H_2O)_{66-n}^{(54-n)+}$ (n = 42–54)	13	$Al_{18}(OH)_{42}(H_2O)_{24}^{12+}$–$Al_{18}(OH)_{54}(H_2O)_{12}^0$
19	Al_{19}	5-ring	$Al_{19}(OH)_n(H_2O)_{68-n}^{(57-n)+}$ (n = 46–57)	12	$Al_{19}(OH)_{46}(H_2O)_{22}^{11+}$–$Al_{19}(OH)_{57}(H_2O)_{11}^0$
20	Al_{20}	5-ring	$Al_{20}(OH)_n(H_2O)_{72-n}^{(60-n)+}$ (n = 48–60)	13	$Al_{20}(OH)_{48}(H_2O)_{24}^{12+}$–$Al_{20}(OH)_{60}(H_2O)_{12}^0$
24	Al_{24}	7-ring	$Al_{24}(OH)_n(H_2O)_{84-n}^{(72-n)+}$ (n = 60–72)	13	$Al_{24}(OH)_{60}(H_2O)_{24}^{12+}$–$Al_{24}(OH)_{72}(H_2O)_{12}^0$
30	Al_{30}	9-ring	$Al_{30}(OH)_n(H_2O)_{104-n}^{(90-n)+}$ (n = 76–90)	14	$Al_{30}(OH)_{76}(H_2O)_{28}^{14+}$–$Al_{30}(OH)_{90}(H_2O)_{14}^0$
42	Al_{42}	13-ring	$Al_{42}(OH)_n(H_2O)_{144-n}^{(126-n)+}$ (n = 108–126)	19	$Al_{42}(OH)_{108}(H_2O)_{36}^{18+}$–$Al_{42}(OH)_{126}(H_2O)_{18}^0$
52	Al_{54}	19-ring	$Al_{54}(OH)_n(H_2O)_{180-n}^{(162-n)+}$ (n = 144–162)	18	$Al_{54}(OH)_{144}(H_2O)_{36}^{18+}$–$Al_{42}(OH)_{162}(H_2O)_{18}^0$

Some important literature relating to the specific descriptions for the various monomeric and polynuclear Al species: Al_1 [2,87,94,96,97]; Al_2 [2,47,53,54,57,70,73,87,98–100]; Al_3 [30,34,36,58,71,87,89,93,96,98]; Al_4 [41,49,89]; Al_5 [73]; Al_6 [37,40,42,43,46,49,88]; Al_7 [37,52,68,77,83,102–104]; Al_8 [2,40,43,49,57,77,105–107]; Al_9 [43,88,108]; Al_{10} [49,51,109]; Al_{11} [22]; Al_{12} [96]; Al_{13} [2,16,19,43,46,49,52–59,73,77,80,89,90,94,98–100,104,108–113]; Al_{14} [52,87,113]; Al_{15} [2,87]; Al_{16} [110]; Al_{17}–Al_{54} [2,16,19,46,48,49,61,66,109,110,114–117].

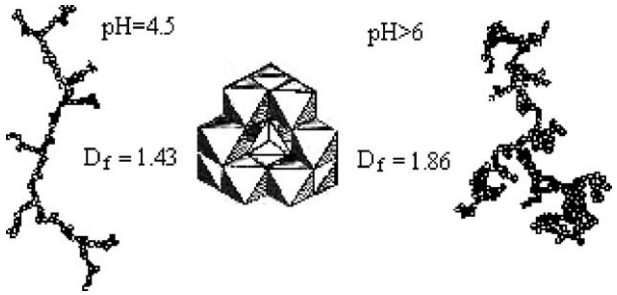

Fig. 7. The model for Al_{13} and its aggregation. D_f is the dispersion coefficient [23].

tween the "Core-links" model Al forms and the "Cage-like" K-Al_{13} species, summarized as C-Al_{13} → K-Al_{13}, which is an irreversible self-assembly. As transient polymeric Al species age, the Al_b(photometry) ≈ K-Al_{13} (^{27}Al-NMR, $\tilde{n} = 0.8$–2.8) shows the existence of K-Al_{13}. Nevertheless, the K-Al_{13} model cannot explain the whole process of formation and transformation of polynuclear Al in solution, as it does not account for species that cannot be detected by ^{27}Al-NMR.

3.2.1. The polymeric Al_b assigned as K-Al_{13}

^{27}Al-NMR and Al-Ferron timed spectrophotometry show that Al_b becomes K-Al_{13} on aging for 1–5 days [13,21,71,118]. Aveston's [100] ultracentrifuge result indicates that polymeric Al solutions of high $\tilde{n}$ values contain only one polymeric species, the highly symmetric ion $Al_{13}O_4(OH)_{24}(H_2O)_{12}^{7+}$. Some researchers [71,118,119] have analyzed the Al-Ferron dynamic reaction and arrive at the same conclusions as Brosset et al. [43], Turner and coworkers [120,121] and Letterman and Asolekar [52]. Concentration of $Al_T = 1 \times 10^{-3}$ M gives two more stable polynuclear Al species when titrated with base. A smaller one with $\tilde{n}$ less than or equal to 2.5 and a larger one with $\tilde{n}$ of $2.5 < \tilde{n} < 2.8$. ^{27}Al-NMR showed the former to be K-Al_{13}, and the latter is the Al_{13} cluster or Al_{13} aggregation (Fig. 7) Alp_2 or $Al_{24}O_{72}$ (a 'defective' Al_{13} dimer [60,70,74,81] resulting from condensation of two Keggin ions, each of which loses a monomer [122]). The mean radius of K-Al_{13} is approximately 12 Å, measured by the small-angle X-ray scattering [112].

3.2.2. Metastable K-Al_{13} formed on aging

Aging is one prerequisite for K-Al_{13} formation that is promoted at elevated temperatures and with addition of extra SO_4^{2-}. The aging time for K-Al_{13} is 1–5 days [64,74] and the changes in content are illustrated by ^{27}Al-NMR spectroscopy in Fig. 8. At 80 °C, the maximum K-Al_{13} content requires 4–8 h aging time. Rausch and Bale [56] studied solutions, with $\tilde{n} = 1$–2.5 immediately after preparation and also in the final equilibrium condition. Aggregates present in freshly prepared solutions probably have a characteristic platelet shape. When aged, these sheet polymers possess a rotary radius similar to K-Al_{13}, so that transient polymeric

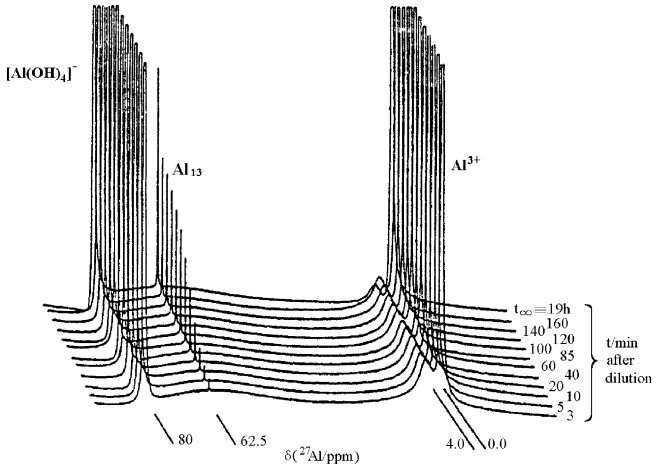

Fig. 8. The evolution of the 104.2 MHz ^{27}Al-NMR spectrum of polymeric Al with time. The solution was prepared by rapid 10-fold dilution of a 1.0 M $AlCl_3$ solution previously base hydrolyzed to $\tilde{n} = 1.0$ at ambient temperature. The low-field resonance of $Al(OH)_4^-$ was used as a quantitative standard and the high-field resonance of the monomer did not change in intensity, enabling truncation of these peaks [73].

Al species is converted into the metastable K-Al_{13}. Bertsch et al. [71] demonstrated that a continual linear increase in Al_{13} concentration would occur up to $\tilde{n} = 2.5$ when the base injection rate was decreased from 1.2 to 0.6 cm^3/min. The percentage of Al_{13} in total Al (Al_T) and $\tilde{n}$ have a linear relation: $Al_{13} = (\tilde{n}/2.46) \times 100$ [13]. Table 3 gives the formation conditions of Keggin-Al_{13} summarized from previous literature.

3.2.3. The polymeric Al_b(photometry) ≈ K-Al_{13}(^{27}Al-NMR) after aging of transient polymeric Al species

After aging, the amount of polymeric Al_b surveyed by photometry and the amount of K-Al_{13} surveyed by ^{27}Al-NMR are essentially equal [13,21,71,118,121], although some differences are observed in partially neutralized solutions with different $\tilde{n}$ values [58,72,101,123], indicating that both models could coexist [66]. However, it is possible that samples tested by different people are in different stages of the formation chain "Al^{3+} → the "Core-links" species (transient form) → K-Al_{13} (metastable) → $Al(OH)_3$ (s, stable state) → $Al(OH)_4^-$".

3.2.4. The self-assembly conversion of C-Al_{13}^{9+} → K-Al_{13}^{7+}

Polymeric Al whose $\tilde{n}$ is 0.8–2.5 age to give K-Al_{13} [20,58,74,124]. In general, the small/middle polymeric Al with relatively small $\tilde{n}$ seize OH^- from coordinated water during aging and continue to polymerize or copolymerize, and the large polymeric Al undergo fasculation during aging. The transient polymeric Al species first form the relatively stable C-Al_{13}, which is the most stable species among panel polymeric Al species [125]. It then self-assembles into three-dimensional K-Al_{13} during aging with corresponding decrease in pH and a formation of new OH^- bridges

Table 3
The formation conditions of Keggin-Al_{13}

Order	Al^{3+} concentration (M)	OH^- concentration (M)	OH/Al mol ratio	Neutralization rate (ml/min)	Temperature (°C)	Aging time of polyaluminum	Aging time after adding SO_4^{2-}	Reference
1	10^{-4} to 10^{-2}	–	0.8–2.4	0.0033–0.33	25	Aging again 1 day after dropping base 4.5 h–20 days	WD	[13]
2	0.2	0.64	2.45	0.05	AT	Aging again 3 days after dropping base 8.5 days	–	[79]
3	0.01–0.2	0.45–2.0	2.3	0.28–0.44	25	1 day	WD	[20]
4	0.1	0.1	1–2.5	1	AT	3–3925 days	WD	[14]
5	0.1	0.1	2.0	1	AT, 45, 60, 75, 90	>5 days	WD	[15]
6	0.125	0.1	2.0	–	45	Aging 1 h under 45 °C	WD	[80]
7	0.1	–	2.0–2.5	1	87	1 day	WD	[64]
8	0.1	0.1	2.2	1	23	5 days	12 days	[78]
9	0.2	0.44	2.2	2	AT	7 days	–	[81]
10	0.1	–	2.2	1.7	22	1 days	WD	[58]
11	0.25	0.25	2.4	4	80	2 days	–	[82]
12	0.25	0.25	2.4	12	75	–	–	[83]
13	2.0	0.5	2.2	Slow	AT	1 day	17 h	[84]
14	0.1	4.0	–	Slow	95	–	7 days	[19]
15	0.02	–	2.2	–	AT	10 days	–	[63]
16	0.75	1.0	2.5	–	90	Aging 1 h under 100 °C	WD	[57]
17	1.0	–	1–2.5	–	70	Aging 1 h under 70 °C	WD	[56]
18	0.5	0.5	2.2	–	80	–	42 days	[85]
19	0.2	0.5	1.0–2.5	0.04	80	1 day	WD	[37]
20	0.25	1	0.8–2.5	–	80	Aging 2 days under 80 °C	WD	[74]

(–) Not mentioned in documents; WD: without injecting SO_4^{2-}; AT: stands for room temperature.

[126]. The larger $\tilde{n}$, the longer the aging time to form K-Al_{13}. The Al_c content in solution after aging will also increase:

$$Al_{13}(OH)_{30}(H_2O)_{18}{}^{9+}(\text{C-}Al_{13}) \rightarrow AlO_4Al_{12}(OH)_{24}(H_2O)_{12}{}^{7+}(\text{K-}Al_{13}) + 8H_2O + 2H^+$$

Colorless prismatic structure $Al_{30}O_8(OH)_{56}(H_2O)_{24}\cdot(SO_4)_9\cdot xH_2O$ was afforded by adding NaOH into a stirred solution of Al^{3+} at 80 °C over a period of 2 h and aged at 80 °C for 3 days [16]. The same Al_{30} species was synthesized by Allouche et al. [19] after aging, consistent with the initial synthesis of K-$Al_{13}{}^{7+}$ by Johansson [53–55].

3.3. The self-assembly of sol/gel and sediment species and the formation of crystalline Al(OH)$_3$—the mechanism of flocculation and precipitation of polynuclear Al species

When $\tilde{n} < 2.8$, aging gives K-Al_{13} prior to the formation of the amorphous or crystal Al hydroxide in partially neutralized Al solutions. The conversion from K-Al_{13} to amorphous Al_c, and then to crystal $Al(OH)_3$ involves self-assembly. The amorphous or crystalline Al hydroxide is formed through a surface coordination process or a gradual growth process from little $[Al(OH)_3]_n$ ($n = 2$–12, aqueous) to sediment $[Al(OH)_3]_n$ ($n \rightarrow \infty$, amorphous or crystalline). Insoluble Al hydroxide sediment begins to deposit at pH 4 and ends at pH 7 [2]. Alternatively, K-Al_{13} self-assembles in the course of aging. Further aging causes the progressive formation of Alp_2 [74], which is necessary for K-Al_{13} to give Al_c, but K-Al_{13} is structurally different from $[Al(OH)_3]_n$ (or Al_c). Although transformation of K-Al_{13} to the more stable Al_c is a general phenomenon, transformation into homogeneous octahedral structure of $[Al(OH)_3]_n$ is not understood [2,23,59], and is the focus of two models:

(1) Adoption of a central AlO_4 tetrahedron or AlO_6 octahedron of K-Al_{13} depends on pressure [127], temperature [128]and the presence of anions such as SO_4^{2-} [2,49,51,67]. Transformations involve both self-assembly of the Keggin ions [129] and the functional replacement [130]. As functional replacement is a specific form of self-assembly, the two theories are unified.
(2) The transformation from this unstable K-Al_{13} complex to the more stable gel or crystal $Al(OH)_3$-fragment structure is very slow at room temperature [15], and irreversible. Gibbsite is observed in the partially neutralized Al solution for $AlCl_3 = 0.02$ M and $\tilde{n} = 2.5$ after aging for at least 6 months at RT [14] or 20 days at 60 °C [131], but after only 8 h in the neutralized Al solution for $AlCl_3 = 0.15$ M and $\tilde{n} = 3.0$. Evidently, the generation rate of Al_c depends on Al^{3+} concentration, $\tilde{n}$, aging temperature, and aging time, etc.

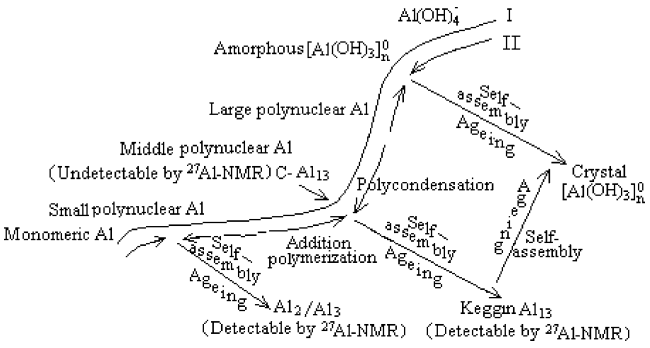

Fig. 9. The "Continuous" model describing the change of Al species directly with a species chain under forced hydrolysis–polymerization of Al^{3+} salts.

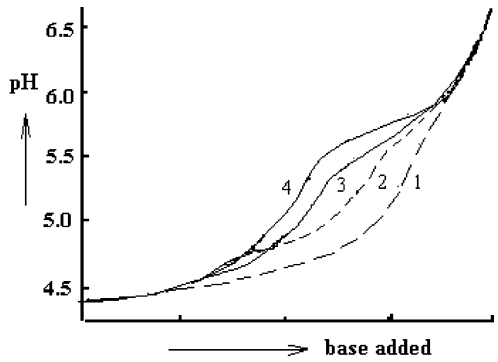

Fig. 10. The effect of base addition on the shape of the pH curve at 25 °C [135]: (1) fast drop-wise addition (5 ml/min); (2) slow drop-wise addition (1.8 ml/min); (3) fast injection (10 ml/min); (4) slow injection (1 ml/min).

(3) The isoelectric point (pH 6.5–7.0) of Al hydroxide is not easy to determine, There is electron microscopic evidence for Al hydroxide particles of 50 nm size [132] with a well-defined hexagonal crystal pattern resembling gibbsite. Al hydroxide may crystallize as bayerite, gibbsite or nordstrandite, which are distinguished by the stacking of bilayers along the *c*-crystallographic axis [47]. The interaction between the (0 0 1) sheets is largely due to weak hydrogen bonding and van der Waals forces. Scanning electronic microscopy crystal structural views of gibbsite and bayerite by are shown in literature [49,110,133,134].

3.4. The "Continuous" model

Differences in preparation conditions, instruments and other procedures have lead to various conclusions regarding hydrolysis–polymerization reaction of Al^{3+}. The "Core-links" model applies to the hydrolysis polymerization of Al^{3+} salt with moderate rate of titration, while the "Cage-like" model applies to the transient polymeric Al from disorder to order. In this section, we present our novel combined "Continuous" model to unify these two models with introducing the concept of the flux of alkali neutralization Φ.

3.4.1. The " Continuous" model—a depiction of the Al species chain under forced hydrolysis, reflecting all stages of polymerization for Al^{3+} salt solutions

Fig. 9 depicts the proposed "Continuous" model. Path I represents the "Core-links" model involving transient polymeric Al species. Through self-assembly, the more stable species after aging are Al_2, K-Al_{13}, Al_{13} and $[Al(OH)_3]_n$(S). $[Al(OH)_3]_n$(S) can be characterized by solid state ^{27}Al-NMR spectroscopy or the X-ray diffraction. Other forms, including $Al(OH)_4^-$, can be measured by solution ^{27}Al-NMR spectroscopy. Akitt et al. [57] proposed the existence of $Al(H_2O)_6^{3+}$, $Al_2(OH)_2(H_2O)_8^{4+}$, $Al_8(OH)_{20}(H_2O)_x^{4+}$, and $Al_{13}O_4(OH)_{24}(H_2O)_{12}^{7+}$ in hydrolyzed Al solutions, as well as the K-Al_{13} cation and small amounts of dimeric and monomeric hexaaqua Al [71,72,135]. Under forced hydrolysis–polymerization of Al^{3+} salts, the changes of Al species can be described directly with a species chain shown in Fig. 9, explaining the mechanism of "hydrolysis–polymerization–flocculation–sediment", series of dynamic intermediates, and the experimental observation of "Al_b(photometry) ≈ K-Al_{13}(^{27}Al-NMR)". The "Continuous" model unifies the "Core-links" model and the "Cage-like" Keggin-Al_{13} model.

3.4.2. The flux of alkali neutralization Φ

The distribution of Al forms in partially neutralized Al solutions depends on many parameters including the concentration of base and Al^{3+}, $\tilde{n}$ value, the neutralization rate, the time of sample preparation and the aging time [2]. In order to unify these experimental conditions, we introduce the "flux of alkali neutralization Φ", parameter that refers to the total amount of base added in unit time to achieve certain basicity. The relative flux of alkali neutralization Φ_r is also introduced to denote the amount of OH^- per mole Al^{3+} in unit time to reach a certain basicity. Φ and Φ_r influence the hydrolysis–polymerization process and

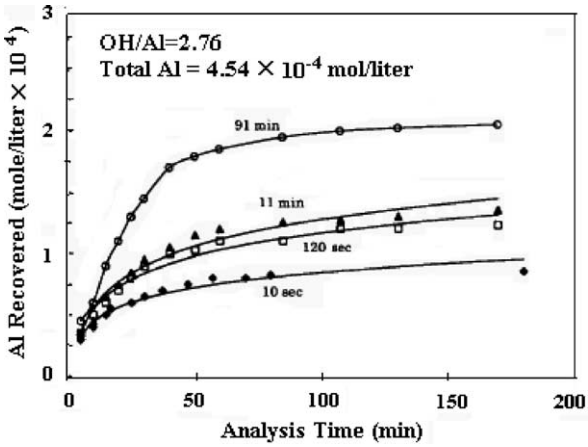

Fig. 11. Effect of the neutralization rate (the time of injecting base) on the amount of Al_a, Al_b, Al_c formed in partially neutralized Al^{3+} solutions ($Al_T = 4.54 \times 10^{-4}$ M; OH/Al = 2.76) [65].

Table 4
Distribution of the Al_{13} polymer in various partially neutralized Al solutions [72]

No.	[Al $^{3+}$] (M)	$\tilde{n}$	Base injection rate (ml/min)	Al_{13}[a]	Comments	Reference
1	1×10^{-1}	≥0.50	3.33	+		[58]
2	1×10^{-1}	>0.5, ≤2.2	3.33	+	Continual linear increase in Al_{13} concentration	[58]
3	1×10^{-1}	>2.2	3.33	+	Concentration of Al_{13} decreased with $\tilde{n}$	[58]
4	3.34×10^{-2}	0.25	1.2	−		[71]
5	3.34×10^{-2}	0.25	86.0	−		[72]
6	3.34×10^{-2}	0.40	1.2	+		[72]
7	3.34×10^{-2}	0.50	1.2	+		[71]
8	3.34×10^{-2}	2.5	0.6	+	Continual linear increase in Al_{13} concentration	[71,72]
9	3.34×10^{-2}	2.5	1.2	+	Concentration of Al_{13} decreased compared to $\tilde{n} = 2.25$	[71,72]
10	3.34×10^{-3}	1.0	1.2	−		[72]
11	3.34×10^{-3}	1.5	1.2	+		[72]
12	3.34×10^{-4}	2.5	1.2	−		[72]
13	3.34×10^{-4}	2.5	100.0	+	62.5 ppm peak visible after 12 h run. Continual linear increase in Al_{13} estimated to be $\sim 3.0 \times 10^{-4}$ M	[72]

[a] Indicates the presence or absence of a detectable 62.5 ppm resonance peak indicative of the Al_{13} polymer, respectively.

species distribution of Al^{3+} salts from Al^{3+} to $Al(OH)_3$. The course of polymerization and the content of three kinds of Al species (Al_a, Al_b, Al_c) relate to the values of Φ or Φ_r (see Figs. 10 and 11).

the flux of alkali neutralization : $$\Phi = \frac{m_b}{t} = VM_b$$

the relative flux of alkali neutralization :

$$\Phi_r = \frac{\Phi}{m_a} = \frac{m_b}{m_a} \times \frac{1}{t} = \frac{\tilde{n}}{t}$$

where m_a and m_b are the mole number of Al^{3+} and OH^- in the solution, respectively; M_b is the concentration of base (M); t is the sum of the preparation time t_b for polymeric Al; V is the rate of addition of base (l/min). The units for Φ and Φ_r are mol/min and min^{-1}, respectively.

Low concentrations of Al^{3+} and high neutralization rate go against the formation of K-Al_{13}. As summarized in Table 4, when $\tilde{n} = 0.25$, K-Al_{13} cannot form irrespective of the addition rate of base (number 4 and 5), and the main Al species are Al^{3+} and mononuclear Al. When the concentration of Al is low, that the rate of adding base should be increased to produce K-Al_{13}. Correspondingly, when the Al concentration is high, the rate must reduced to produce K-Al_{13}.

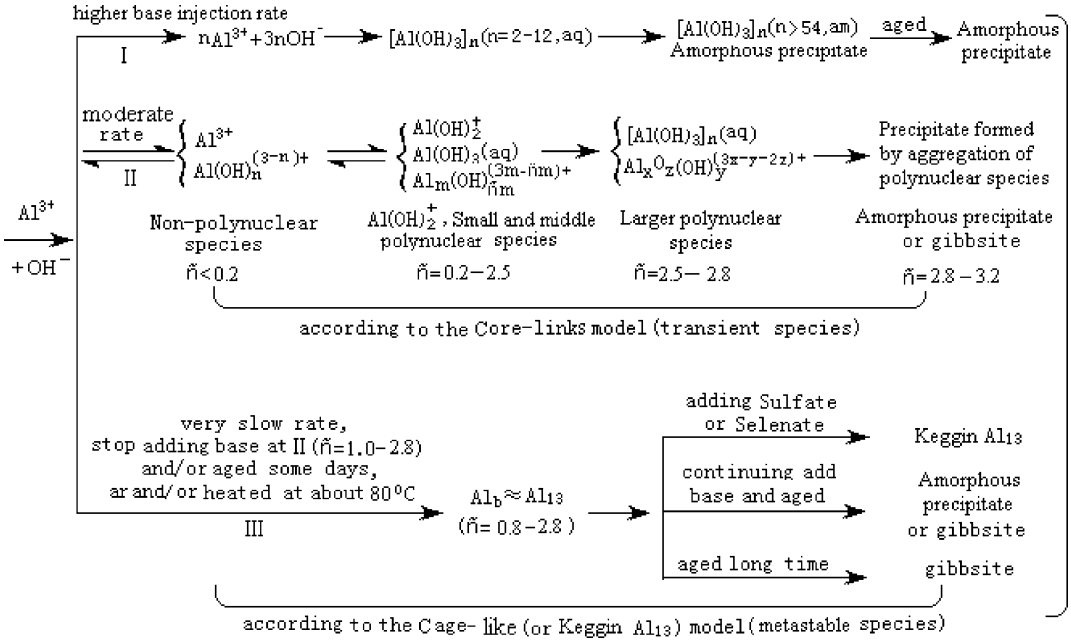

Fig. 12. The effect of the relative flux of alkali neutralization (Φ_r) on the course of hydrolysis–polymerization–flocculation–sediment of Al(III) salts and the proposed pathway for the corresponding Al species conversion.

3.4.3. The effects of the flux of alkali neutralization Φ on "hydrolysis–polymerization–flocculation–sediment" of Al^{3+} salts

Polynuclear Al species are actually a series of dynamic intermediates formed in the process of "hydrolysis–polymerization–flocculation–sediment", and the formation of K-Al_{13} during aging [94] is sensitive to the neutralization rate [51,65,72,131]. Slower neutralization rates promote formation of K-Al_{13}. The flux of alkali neutralization Φ is a pacing factor in the formation, the changing, and the evolution course of polymeric Al species. We have summarized the process with the law of the "hydrolysis–polymerization–flocculation–sediment", as shown in Fig. 12.

In path I, the neutralization rate is so rapid (high Φ_r) that partial supersaturation often occurs and amorphous sediment is formed [49,124,131]. As a result, none or extremely small amounts of K-Al_{13} are formed [63,71,123,124]. In path II involving a moderate neutralization rate (moderate Φ_r), the hydrolysis–polymerization of Al follows the "Core-links" model [22,87,136]. Rausch and Bale [56] used the small angle X-ray scattering to study the hydrolysis–polymerization of $Al(NO_3)_3$ and found that when $\tilde{n} = 1$–2.5, the newly prepared polymeric Al adopts a sheet structure. In path III, the slow neutralization rate (small Φ_r) promotes K-Al_{13} [22,23,71,123], obeying the "Cage-like" model. When polymeric Al solutions of $\tilde{n} = 1.0$–2.5 are aged or heated to make Φ smaller, K-Al_{13} will be formed firstly because the rate of the K-Al_{13}'s formation is faster than the rate of precipitation for $[Al(OH)_3]_n$ [31,137]. When $\tilde{n} > 2.8$, most of the K-Al_{13} becomes aggregated and self-assembles. When $\tilde{n} = 3.0$, $[Al(OH)_3]_n$ sediment forms rather than K-Al_{13}. Studies have shown that the amorphous precipitate of $[Al(OH)_3]_n$ formed in the initial course of aging evolves into crystalline forms [20,47,49,59,63,138–140].

Acknowledgements

This project is supported by the National Natural Science Foundation of China (Nos. 20075011 and 49831005), Research Funding from the MOE of China for Young Teachers at Key University, Hwa-Ying Scholarship of Nanjing University and a Visiting Fellowship from the Berkeley Lawrence National Laboratory of USA.

References

[1] G.H. Robinson, Coordination Chemistry of Aluminum, VCH, 1993.
[2] P.M. Berch, in: G. Sposito (Ed.), The Environmental Chemistry of Aluminum, CRC Press, Boca Raton, FL, 1989, p. 87.
[3] J.P. Pineiro, A.M. Mota, M.F. Benedtti, Environ. Sci. Technol. 34 (2000) 5137.
[4] S.P. Bi, S.Q. An, W. Tang, R. Xue, L.X. Wen, F. Liu, J. Inorg. Biochem. 87 (2001) 97.
[5] K. Pyrzynska, S. Gucer, E. Bulska, Water Res. 34 (2000) 359.
[6] J.M. de la Furnte, V. Ramirez-Rodriguez, J.L. Cabrera-Ponce, L. Herrera-Estrella, Science 276 (1997) 1566.
[7] J.J. Comin, J. Barloy, G. Bourrie, F. Trolard, Eur. J. Agron. 11 (1999) 115.
[8] S. Desroches, S. Dayde, G. Berthon, J. Inorg. Biochem. 81 (2000) 301.
[9] D. Hunter, D.S. Ross, Science 251 (1991) 1056.
[10] E. Gauthier, I. Fortier, F. Courchesne, P. Pepin, J. Mortimer, D. Gauvreau, Environ. Res. Sect. A 84 (2000) 234.
[11] W.J. Lukiw, N.G. Bazan, Neurochem. Res. 25 (2000) 1173.
[12] M.E. Karaman, R.M. Pashley, T.D. Waite, S.J. Hatch, H. Bustamante, Colloids Surf. A: Physicochem. Eng. Aspects 129–130 (1997) 239.
[13] D.R. Parker, P.M. Bertsch, Environ. Sci. Technol. 26 (1992) 908.
[14] W.Z. Wang, P.H. Hsu, Clays Clay Miner. 42 (1994) 356.
[15] P.H. Hsu, Clays Clay Miner. 45 (1997) 286.
[16] J. Rowsell, L.F. Nazar, J. Am. Chem. Soc. 122 (2000) 3777.
[17] M.L. Occelli, J.A. Bertrand, S.A.C. Gould, J.M. Dominguez, Micropor. Mesopor. Mater. 34 (2000) 195.
[18] M.L. Occelli, A. Auroux, G.J. Ray, Micropor. Mesopor. Mater. 39 (2000) 43.
[19] L. Allouche, C. Huguenard, F. Taulelle, J. Phys. Chem. Solid 62 (2001) 1525.
[20] C.C. Perry, K.L. Shafran, J. Inorg. Biochem. 87 (2001) 115.
[21] D.R. Parker, P.M. Bertsch, Environ. Sci. Technol. 26 (1992) 914.
[22] C.Y. Wang, S.P. Bi, M.B. Luo, ACS Symp. Ser., Am. Chem. Soc. (Washington, DC) 822 (2002) 246.
[23] H.X. Tang, Acta Scientiae Circumstantiae 18 (1998) 1 (in Chinese).
[24] F. Thomas, A. Masion, J.Y. Bottero, J. Rouiller, F. Genevrier, D. Boudot, Environ. Sci. Technol. 25 (1991) 1553.
[25] L.O. Ohman, S. Sjoberg, Coord. Chem. Rev. 149 (1996) 33.
[26] A.E. Martell, R.D. Hancock, R.M. Smith, R.J. Motekaitis, Coord. Chem. Rev. 149 (1996) 311.
[27] B.A. Browne, C.T. Driscoll, Science 256 (1992) 1667.
[28] S.P. Bi, X.D. Yang, F.P. Zhang, X.L. Wang, G.W. Zou, Fresenius J. Anal. Chem. 370 (2001) 984.
[29] K. Pyrzynska, E. Bulska, S. Gucer, A. Huianicki, Chem. Anal. (Warsaw) 44 (1999) 1.
[30] Z.K. Luan, Environ Chem. 6 (1987) 46 (in Chinese).
[31] A. Amirbahman, M. Gfeller, G. Furrer, Geochim. Cosmochim. Acta 64 (2000) 911.
[32] E. Lydersen, B. Salbu, in: B.T. Mason (Ed.), Studies of Aluminum Species in Fresh Water: The Surface Water Acidification Program, 1992.
[33] F. Gérard, J.P. Boudot, J. Ranger, Appl. Geochem. 16 (2001) 513.
[34] D. Panias, P. Asimidis, I. Paspaliaris, Hydrometallurgy 59 (2001) 15.
[35] S.L. Simpson, K.J. Powell, N. Nilsson, Anal. Chim. Acta 343 (1997) 19.
[36] C. Exley, Aluminum and Alzheimer's Disease: The Science that Describes the Link, Elsevier, Amsterdam, 2001.
[37] Z.K. Luan, L. Feng, H.X. Tang, Acta Scientiae Circumstantiae 15 (1995) 39 (in Chinese).
[38] Z.K. Luan, H.X. Tang, Environ. Chem. 16 (1997) 497 (in Chinese).
[39] D.J. Wesolowski, D.A. Palmer, Geochim. Cosmochim. Acta 58 (1994) 2947.
[40] Y.Y. Hu, Z.S. Wang, H.X. Tang, Acta Scientiae Circumstaniae 14 (1994) 137 (in Chinese).
[41] J.J. Fripiate, F.V. Cauwelaert, H. Bosmans, J. Phys. Chem. 69 (1965) 2458.
[42] C. Brosset, Acta Chem. Scand. 6 (1952) 910.
[43] C. Brosset, G. Biedermann, L.G. Sillén, Acta Chem. Scand. 8 (1954) 1917.
[44] L.G. Sillén, Acta Chem. Scand. 8 (1954) 299.
[45] P.H. Hsu, C.I. Rich, Soil Sci. Soc. Am. Proc. 24 (1960) 21.
[46] P.H. Hsu, T.F. Bates, Miner. Mag. 33 (1964) 749.

[47] R.J. Stol, A.K. van Helden, P.L. Bruyn, J. Colloid Interface Sci. 57 (1976) 115.
[48] P.M. Huang, Soil Chemistry, Science Press, Beijing, 1991.
[49] P.H. Hsu, On Soil Chemistry, Science Press, Beijing, 1986.
[50] A. Schutz, W.E.E. Stone, G. Poncelet, J.J. Fripiat, Clays Clay Miner. 35 (1987) 251.
[51] P.H. Hsu, in: J.B. Dixon, S.B. Weed (Eds.), Minerals in Soil Environment, second ed., Soil Science Society of America, Madison, WI, 1988.
[52] R.D. Letterman, S.R. Asolekar, Water Res. 24 (1990) 931.
[53] G. Johansson, Acta Chem. Scand. 16 (1962) 403.
[54] G. Johansson, Acta Chem. Scand. 14 (1960) 771.
[55] G. Johansson, Ark. Kemi. 20 (1963) 321.
[56] W.V. Rausch, H.D. Bale, J. Chem. Phys. 40 (1964) 3391.
[57] J.W. Akitt, N.N. Greenwood, B.L. Khandelwal, G.D. Lester, J. Chem. Soc. Dalton. Trans. (1972) 604.
[58] J.Y. Bottero, J.M. Cases, F. Fiessinger, J.E. Poirier, J. Phys. Chem. 84 (1980) 2933.
[59] J.Y. Bottero, M. Axelos, D. Tchoubar, J.M. Cases, J.J. Fripiat, F. Fiessinger, J. Colloid Interface Sci. 117 (1987) 47.
[60] J.W. Akitt, A. Farthing, J. Chem. Soc., Dalton. Trans. (1981) 1606.
[61] L. Allouche, C. Gérardin, T. Loiseau, G. Férey, F. Taulelle, Angew. Chem. Int. Ed. 39 (2000) 511.
[62] J.A. Tosell, Geochim. Cosmochim. Acta 65 (2001) 2549.
[63] D.Z. Denney, P.H. Hsu, Clays Clay Miner. 34 (1986) 604.
[64] C. Changui, W.E.E. Stone, L. Vielvoye, J.M. Dereppe, J. Chem. Soc., Dalton Trans. (1990) 1723.
[65] R.W. Smith, Coord. Chem. Rev. 149 (1996) 81.
[66] P. Capkova, R.A.J. Driessen, M. Numan, H. Schenk, Z. Weiss, Z. Klika, Clays Clay Miner. 46 (1998) 240.
[67] P.H. Hsu, Clays Clay Miner. 36 (1988) 25.
[68] G.J. Lu, J.H. Qu, H.X. Tang, Water Res. 33 (1999) 807.
[69] C.Y. Wang, S.P. Bi, M.B. Luo, Rev. Anal. Chem. 22 (2003) 53.
[70] J.W. Akitt, Progr. Nuclear Magn. Reson. Spectrosc. 21 (Part 1/6) (1989) 1.
[71] P.M. Bertsch, R.I. Barnhisel, G.W. Thomas, W.J. Layton, S.L. Smith, Anal. Chem. 58 (1986) 2583.
[72] P.M. Bertsch, Soil Sci. Soc. Am. J. 51 (1987) 825.
[73] J.W. Akitt, J.M. Elders, J. Chem. Soc., Dalton. Trans. (1988) 1347.
[74] W.O. Parker Jr., I. Kiricsi, Appl. Catal. A: Gen. 121 (1995) L7.
[75] M.P.B. van Bruggen, M. Donker, H.N.W. Lekkerkerker, T.L. Hughes, Colloids Surf. A: Physicochem. Eng. Aspects 150 (1999) 115.
[76] S.M. Bradley, R.A. Kydd, R.F. Howe, J. Colloid Interface Sci. 159 (1993) 405.
[77] E. Matijeviæ, L.J. Stryker, J. Colloid Interface Sci. 22 (1966) 68.
[78] G.S.R. Krishnamurti, M.K. Wang, P.M. Huang, Clays Clay Miner. 47 (1999) 658.
[79] B. Lothenbach, G. Furrer, R. Schulin, Environ. Sci. Technol. 31 (1997) 1452.
[80] G. Furrer, M. Gfeller, B. Wehrli, Geochim. Cosmochim. Acta 63 (1999) 3069.
[81] E. Molis, F. Thomas, J.Y. Bottero, O. Barrés, A. Masion, Langmuir 12 (1996) 3195.
[82] R.A. Schoonheydt, H. Leeman, A. Scorpion, I. Lenotte, P. Grobet, Clays Clay Miner. 42 (1994) 518.
[83] M. Wang, M. Muhammed, Nanostruct. Mater. 11 (1999) 1219.
[84] D.S. Wang, H.X. Tang, Q. Gao, J.L. Shao, Environ. Chem. 19 (2000) 389 (in Chinese).
[85] J.T. Kloprogge, R.L. Frost, Thermochim. Acta 320 (1998) 245.
[86] H. Hek, R.J. Stol, P.L. Bruyn, J. Colloid Interface Sci. 64 (1978) 72.
[87] R.E. Mesmer, C.F. Baes, Inorg. Chem. 10 (1971) 2290.
[88] J.H. Patterson, J.R.S. Tyree, J. Colloid Interface Sci. 2 (1973) 389.
[89] Z.K. Luan, H.X. Tang, Acta Scientiae Circumstaniae 8 (1988) 146 (in Chinese).
[90] P.L. Brown, R.N. Sylva, G.E. Batley, J. Elis, J. Chem. Soc., Dalton Trans. (1985) 1967.
[91] Y.H. Shen, B.A. Dempsey, Environ. Int. 24 (1998) 899.
[92] G. Jander, A. Winker, Z. Anorg. Chem. 200 (1931) 257.
[93] X.Q. Lu, Z.L. Chen, X.H. Yang, Water Res. 33 (1999) 3271.
[94] C.F. Baes, R.E. Mesmer, The Hydrolysis of Cations, Wiley, New York, 1976.
[95] S.P. Bi, Analyst 120 (1995) 2033.
[96] S.S. Lin, W.G. He, Technol. Water Treat. 17 (1991) 162 (in Chinese).
[97] S.P. Bi, Environ. Poll. 92 (1996) 85.
[98] F. Salvatore, M. Trifuoggi, J. Coord. Chem. 51 (2000) 271.
[99] A. Badora, G. Furrer, A. Grunwald, R. Schulin, J. Soil Contam. 7 (1998) 573.
[100] J. Aveston, J. Chem. Soc. 1965 (1965) 4438.
[101] J. Buffle, N. Parthasarathy, W. Haerdi, Water Res. 19 (1985) 7.
[102] J.E. Van Benschoten, J.K. Edzwald, Water Res. 24 (1990) 1519.
[103] J.E. Van Benschoten, J.K. Edzwald, Water Res. 24 (1990) 1527.
[104] H.X. Tang, Environ. Chem. 9 (1990) 1 (in Chinese).
[105] E. Matijević, B. Tezak, J. Phys. Chem. 57 (1953) 951.
[106] E. Matijević, K.G. Mathai, R.H. Ottewill, M. Kerker, J. Phys. Chem. 65 (1961) 826.
[107] P.L. Hayden, A.J. Rubin, in: A.J. Rubin (Ed.), Aqueous–Environmental Chemistry of Metals, Ann Arbor Science, Ann Arbor, MI, 1976.
[108] J.W. Akitt, N.N. Greenwood, B.L. Khandelwal, G.D. Lester, J. Chem. Soc. (1971) 2450.
[109] P. Capkova, R.A.J. Driessen, M. Numan, H. Schenk, Z. Weiss, Z. Klika, Clays Clay Miner. 46 (1998) 232.
[110] J.A. Davis, J.D. Hem, in: G. Sposito (Ed.), The Environmental Chemistry of Aluminum, CRC Press, Boca Raton, FL, 1989, p. 186.
[111] W. Seichter, H.J. Mögel, P. Brand, D. Salah, Eur. J. Inorg. Chem. (1998) 795.
[112] J.Y. Bottero, D. Tchoubar, M. Cases, F. Flessinger, J. Phys. Chem. 86 (1982) 3667.
[113] D.D. Macdonald, P. Butler, D. Owen, J. Phys. Chem. 77 (1973) 2474.
[114] N. Parthasarathy, J. Buffle, Water Res. 19 (1985) 25.
[115] T.P. Lippa, S.A. Lyapustina, S.J. Xu, O.C. Thomas, K.H. Bowen, Chem. Phys. Lett. 305 (1999) 75.
[116] Q. Sun, Q. Wang, J.Z. Yu, T.M. Briere, Y. Kawazoe, Phys. Rev. A 64 (2001) 3203.
[117] L.G. Sillén, Q. Rev. 13 (1959) 146.
[118] P.P. Tsai, P.H. Hsu, Soil Sci. Soc. Am. J. 49 (1985) 1060.
[119] P.P. Tsai, P.H. Hsu, Soil Sci. Soc. Am. J. 48 (1984) 59.
[120] R.C. Turner, G.J. Ross, Can. J. Chem. 48 (1970) 723.
[121] R.C. Turner, Can. J. Chem. 54 (1976) 1910.
[122] W.O. Parker Jr., R. Millini, I. Kiricsi, Inorg. Chem. 36 (1997) 571.
[123] L. Feng, H.X. Tang, Adv. Environ. Sci. 6 (1997) 44 (in Chinese).
[124] A.R. Thompson, A.C. Kunwar, H.S. Gutowsky, E. Oldfeld, J. Chem. Soc., Dalton Trans. (1987) 2317.
[125] L.G.M. Pettersson, C.W. Bauschlicher, H. Halicioglu, J. Chem. Phys. (1987) 2205.
[126] G. Furrer, C. Ludwig, P.W. Schinlder, J. Colloid Interface Sci. 149 (1992) 56.
[127] J.Y. Bottero, J. Phys. IV 3 (1993) 211.
[128] M.S. Peng, D.E. Li, E. Zhang, J.P. Peng, Acta Mineral. Sinica 18 (1998) 425 (in Chinese).
[129] A. Drljaca, M.J. Hardie, C.L. Raston, J. Chem. Soc., Dalton Trans. (1999) 3639.
[130] D.N. Ye, D. Pushcharovsky, N.C. Shi, Z.S. Ma, Z. Li, Sci. China (Seri. D) 31 (2001) 938.
[131] K.P. Prodromou, A.S. Pavlatou-Ve, Clays Clay Miner. 43 (1995) 111.

[132] J.D. Hem, Adv. Chem. Ser. 106 (1971) 98.
[133] W.H. Casey, B.L. Phillips, M. Karlsson, Geochim. Cosmochim. Acta 64 (2000) 2951.
[134] K.A. Blanks, J. Cryst. Growth 220 (2000) 572.
[135] J.W. Akitt, A. Farthing, J. Magn. Reson. 32 (1978) 345.
[136] N.B. Milic, Z.D. Bugarcic, P.T. Djurdjevic, Can. J. Chem. 69 (1991) 28.
[137] G. Furrer, B. Trusch, C. Müller, Geochim. Cosmochim. Acta 56 (1992) 3831.
[138] A. Violante, P.M. Huang, Clays Clay Miner. 41 (1993) 590.
[139] M. Digne, P. Sautet, P. Raybaud, H. Toulhoat, E. Artacho, J. Phys. Chem. B 106 (2002) 5155.
[140] S.J. Duffy, G.W. van Loon, Environ. Sci. Technol. 28 (1994) 1950.